Predictive Modeling of Phenol Chemical Potentials in Molten Bisphenol A−Polycarbonate over a Broad Temperature Range

Berk Hess and Nico F. A. van der Vegt*

Max Planck Institute for Polymer Research, Ackermannweg 10, D-55128 Mainz, Germany

Received July 9, 2008
Revised Manuscript Received September 1, 2008

The knowledge of infinite-dilution solvent activities in molten polymers is essential for many processes in polymer production and purification. Theoretical approaches that reach the accuracy of experiments are urgently needed, not only to replace expensive experiments but also to improve our atomic-level understanding of complex materials systems, including thin-film protective or barrier coatings, where activity coefficients of solvents and other impurities need to be understood in relation to the polymer chemistry, local chain packing, and system morphology.

In a recent publication we reported a nonequilibrium free energy sampling method applied to calculate excess chemical potentials (ECPs) of solvents in polymers.[1] By running multiple fast-growth thermodynamic integrations (FGTI) in parallel, highly accurate estimates of propane, chloroform and dimethyl sulfoxide ECPs were obtained in a liquid of bisphenol A−polycarbonate (BPA−PC) 5-mers. ECPs were obtained from Jarzynski's identity;[2] i.e., the free energy difference is expressed as an exponential average of the work performed on the system during irreversible transformations. Given the (small) inaccuracy in the computed data obtained with this method,[1] validation of the force field for these types of chemically complex systems has come into reach. Here, we report the calculation of infinite-dilute phenol ECPs in entangled, monodisperse BPA−PC melts with $M_n = 5294$ g/mol. This molecular weight corresponds to 20 chemical repeat units (we model phenoxy end groups) and is close to molecular weights examined experimentally.[3] We note that the above molecular weight corresponds to ∼4 entanglement lengths.[4] The all-atom BPA−PC systems have been prepared by inverse mapping of equilibrated coarse-grained melts.[5] The polycarbonate/phenol system is important in high-conversion polymerization of polycarbonate where it is necessary to remove phenol, formed upon transesterification of diphenylcarbonate with bisphenol A. The temperatures examined in our simulations range between 573 K (high-temperature melt) and 423 K (the experimental T_g).

For the computational details, the reader is referred to the Supporting Information. The work distributions at 423, 473, and 573 K are shown in Figures 1 and 2. The first thing to notice from the distributions is that the spread is strongly temperature dependent. The glass transition temperature of BPA−PC is close to 423 K, where it is "difficult" to insert additive molecules, because the dynamics of the matrix is very slow. At 573 K the matrix is liquidlike, and the insertion is so easy that the spread in the distribution is less than k_BT. In the plots also the exponentially reweighted distributions are shown. At 423 and 473 K these distributions suddenly stop on their low-energy sides, which shows that there is not enough sampling. At 423 K only a few simulations determine the value of the ECP. To be more specific, Jarzynski's formula[2] can be split into two terms:

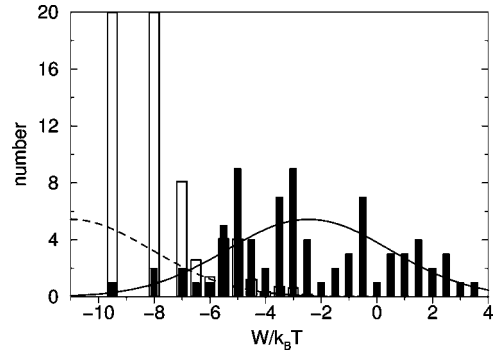

Figure 1. Work distribution for the coupling of a phenol molecule at 423 K. The coupling time for each of the FGTI runs is 2.2 ns. The empty bars show the exponentially reweighted distribution. The solid line is a Gaussian curve with average $\langle W \rangle$ and standard deviation $\sigma(W)$. The dashed line is the same Gaussian curve shifted by $-\beta\sigma^2$.

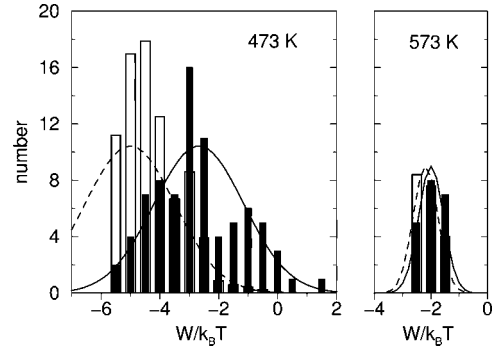

Figure 2. As Figure 1, but for 473 and 573 K.

$$\mu_{ex} = -k_B T \log\langle e^{-\beta W}\rangle = -k_B T \log \sum_{i=1}^{N} e^{-\beta W_i} + k_B T \log\ N \tag{1}$$

Here, μ_{ex} is the ECP, the angular brackets denote a canonical average over the initial (uncoupled) state, $\beta = (k_BT)^{-1}$, and W_i is the coupling work of the ith FGTI run. The sum runs over all N FGTI runs. Work values which are several k_BT higher than the lowest values only contribute to the log N term, not to the first term. To quantify how many "relevant" simulations, i.e., that contribute to the first term, have been performed, one can look at the weighted average of the weights. The inverse of this average weight gives the effective number of simulations: For equilibrium free energy calculations (which are computationally infeasible for this system) all weights are equal and N_e becomes equal to N. In Table 1 the effective number of simulations is given. At 423 K, effectively only 5% of the simulations contribute to the ECP. Here we could have improved the efficiency significantly by moving the system slower from

$$\frac{1}{N_e} = \sum_{i=1}^{N} \left(\frac{e^{-\beta W_i}}{\sum_{j=1}^{N} e^{-\beta W_j}} \right)^2 \tag{2}$$

* To whom correspondence should be addressed.

10.1021/ma8015486 CCC: $40.75
Published on Web 09/23/2008

Table 1. ECP μ_{ex} at Three Temperatures T Obtained from N Fast-Growth Simulations[a]

T (K)	N	N_e	$\beta\sigma$	μ_{ex}^G (kJ/mol)	μ_{ex} (kJ/mol)	Δ_B (kJ/mol)	Δ_G (kJ/mol)
423	80	4	2.9	−23.7	−20.2	1.8	4.5
473	80	29	1.5	−15.1	−14.0	0.6	1.2
573	20	17	0.4	−10.0	−10.0	0.5	0.5

[a] N_e is the effective number of simulations (see text). Also shown is the ECP for a Gaussian distribution μ_{ex}^G with standard deviation σ; $\beta = (k_BT)^{-1}$; Δ_B is the bootstrap error estimate, and Δ_G is an error estimate assuming a Gaussian distribution. See the text for details.

Table 2. Comparison of Calculated ECPs with Experiment in Units of kJ/mol[a]

T (K)	exp 1	exp 2	simulation
423	−20.4		−20 ± 4
473	−18.1	−16.6	−14 ± 1
573	−13.8		−10.0 ± 0.5

[a] Exp 1 is by S. W. Webb;[7] exp 2 is by R. Baltus in ref 7.

the initial (uncoupled) state to the final (coupled) state. At the higher temperatures the efficiency is good.

In general, one does not know what one has not sampled. But since the work distributions are similar to Gaussians, we can get a rough estimate of the systematic error due to the lack of sampling by comparing the ECPs to those for pure Gaussian distributions.[1] For a Gaussian distribution the reweighting produces again a Gaussian distribution which is shifted by $-\beta\sigma^2$. By comparing with the reweighted Gaussian in Figures 1 and 2, one can see that there indeed seems to be a lack of sampling, especially at 423 K. To obtain the ECP, μ_{ex}^G, corresponding to a Gaussian distribution, we only need the average and the standard deviation of the work distribution:

$$\mu_{ex}^G = \langle W \rangle - \frac{1}{2}\beta\sigma^2 \tag{3}$$

The second term gives the irreversible work, which is proportional to the variance of the distribution. In Table 1 one can see that at 423 K there is a discrepancy of about k_BT between the two ECPs. At 473 K the difference is smaller but noticeable, whereas at 573 K only 20 simulations provide enough sampling. This can also be seen from the error estimate in Table 1. We performed a bootstrap error estimate, which (incorrectly) assumes that the sampled distribution over N simulations is correct and an error estimate assuming a Gaussian distribution with standard deviation σ; for both error estimates we averaged a million realizations. The two methods produce significantly different error estimates, except at the highest temperature. Despite the fact that the sampled work distributions and the Gaussian work distributions are quite similar (see Figures 1 and 2), application of the bootstrap procedure to the Gaussian distribution will give a larger variance in the resulting distribution of ECP values due to the exponential weighing of the low energy tail. The Gaussian error estimates Δ_G seem more realistic than the bootstrap error estimates Δ_B as they are closer to the observed differences $\mu_{ex} - \mu_{ex}^G$.

In most cases, the initial and final states are known, and forward and reverse coupling processes may be performed to improve the accuracy of the free energy calculation using Crooks relation.[6] In our case, the systematic error is however mostly determined by insufficient sampling of low-energy minima of the end state. Reversing the integration process from one of the few sampled minima will not lead to sampling additional work values in the low-energy tail of the work distribution.

Experimentally, ECPs of additive molecules in polymers can be determined with inverse gas chromatography. In Table 2 we show a comparison with two experiments.[7] The two experimental ECPs at 473 K differ by 1.5 kJ/mol, which is more than the computational accuracy of the simulations. The simulations at the two higher temperatures overestimate the ECPs (are too positive) by ~4 kJ/mol. The excess enthalpy can be determined from the temperature dependence of the ECP. For the experiment this gives −34 kJ/mol at 473 K. The simulation gives the same enthalpy within the accuracy of the derivative between 473 and 573 K, which is 7 kJ/mol. It has however been shown that the BPA−PC force field used in this work underestimates the heat of vaporization of bisphenol A by 5%.[8] Also, the phenol force field used in our calculations underestimates the phenol heat of vaporization by a few percent for the temperatures examined here.[9] This is consistent with the overestimation of the phenol ECP in BPA−PC. An increase of the interaction strength of the Lennard-Jones and/or charge interactions in the force field by a few percent would solve this issue. It is worth noting that at 573 K in the NPT ensemble with the 2.5% too high density (for details see Supporting Information) the ECP increases by 1.8 kJ/mol. Although this is less than the current difference between experiment and simulation, the effect is larger than the computational accuracy of the simulations. This shows that for accurate predictions of ECPs not only an accurate parametrization of the interaction energies is required but also an accurate description of the melt density.

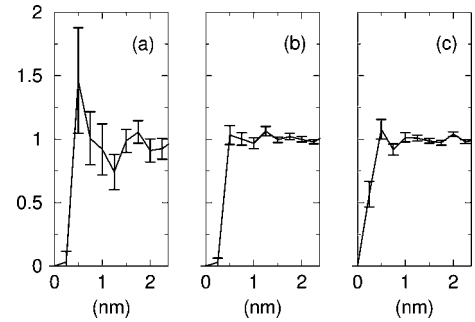

Figure 3. Phenol−polymer radial distribution functions at 473 K: (a) phenol COM−last three carbons in both BPA−PC phenyl end groups; (b) phenol COM−BPA−PC methyl groups; (c) phenol oxygen−BPA−PC carbonyl oxygen.

In previous work we have shown that propane has a preference to reside at the end groups of BPA−PC, whereas dimethyl sulfoxide has no preference.[1] We have looked at solute−polymer radial distribution functions (RDFs) at 473 K, where we effectively have 29 fully coupled conformations and a reasonably sampled work distribution. The RDFs are shown in Figure 3. For the center of mass (COM) of phenol with the end groups of BPA−PC the RDF is 1.5 between 0.5 and 0.6 nm. However, this high value is the result of only two simulations with work values at the lower end of the distribution. Without these two simulations the RDF is 1 within the error margins. We also looked at the RDF of phenol with the methyl carbons of the isopropylidene units in BPA−PC and the hydroxyl group of phenol with the carbonate groups in the BPA−PC. Also, there RDFs are equal to 1 within the error margins, indicating that preferential interactions with the polymer backbone are absent at this temperature. Therefore, we conclude that there might be a slight preference for phenol to occupy locations close to the end groups of BPA−PC, but an order of magnitude more simulations are required to resolve this question with certainty.

Using the same procedure as described above, we also determined the ECP of water in BPA−PC. We chose the simple point charge water model.[10] At 473 K we performed 40 simulations which resulted in a ECP of 5.4 kJ/mol with

a bootstrap and Gaussian error estimate of 0.5 kJ/mol. The experimentally reported ECP is −6 kJ/mol.[7] The discrepancy between simulation and experiment is far too large to be fully attributed to force field issues. We therefore suspect that water reacts with BPA−PC, which is a well-known cause of polycarbonate degradation.

In conclusion, we have shown that fast-growth simulations can efficiently be used to perform predictive modeling of ECPs of additive molecules in polymer matrices. The method is well-suited to be used in combination with all-atom molecular dynamics simulations of polymers with complex chemical topologies. FGTI overcomes the sampling problems usually encountered with the insertion of large and rigid (e.g., aromatic) solvent molecules in dense polymer melts. Accuracies higher than 1 kJ/mol can be achieved over a broad range of temperatures. Only very close to the glass transition temperature the dynamics of the polymer matrix becomes too slow to achieve reasonable accuracies. For many systems the accuracy of the force field will be the limiting factor to predictively model solute ECPs. In such cases, the presented methodology can be used to improve the force field model at a state point where experimental data are available. The FGTI method can then be used for predictive modeling of polymer−solvent phase equilibria in a broader range of thermodynamic conditions.

Acknowledgment. The authors thank Kurt Kremer for many fruitful discussions on the BPA−PC system and Vagelis Harmandaris and Jon Halverson for carefully reading the manuscript.

Supporting Information Available: Methods and computational details. This material is available free of charge via the Internet at http://pubs.acs.org.

References and Notes

(1) Hess, B.; Peter, C.; Ozal, T.; van der Vegt, N. F. A. *Macromolecules* **2008**, *41*, 2283–2289.
(2) Jarzynski, C. *Phys. Rev. Lett.* **1997**, *78*, 2690–2693.
(3) Sadowski, G.; Mokrushina, L. V.; Arlt, W. *Fluid Phase Equilib.* **1997**, *139*, 391.
(4) León, S.; van der Vegt, N.; Delle Site, L.; Kremer, K. *Macromolecules* **2005**, *38*, 8078–8092.
(5) Hess, B.; Leon, S.; van der Vegt, N.; Kremer, K. *Soft Matter* **2006**, *2*, 409.
(6) Crooks, G. E. *Phys. Rev. E* **1999**, *60*, 2721–2726.
(7) Webb, S. W. *AIChE J.* **1993**, *39*, 701–706.
(8) Hahn, O.; Mooney, D. A.; Müller-Plathe, F.; Kremer, K. *J. Chem. Phys.* **1999**, *111*, 6061.
(9) Mooney, D. A.; Müller-Plathe, F.; Kremer, K. *Chem. Phys. Lett.* **1998**, *294*, 135–142.
(10) Berendsen, H. J. C.; Postma, J. P. M.; van Gunsteren, W. F.; Hermans, J. Interaction Models for Water in Relation to Protein Hydration. In *Intermolecular Forces*; Pullman, B., Ed.; D. Reidel Publishing Co.: Dordrecht, 1981.

MA8015486